0.63μ Scatter Measurements from Teflon* and Various Metallic Surfaces

By R. A. SEMPLAK

(Manuscript received May 27, 1965)

Angular scatter measurements obtained by illuminating Teflon and various metallic surfaces at normal incidence with a 0.63μ laser beam are discussed. A method for measuring the scatter in the specular direction is also presented. The measured data are found to be in good agreement with models, which take into account specular reflection, scatter, and absorption. The surfaces investigated were aluminum, steel, brass, first surface aluminized mirror, and aluminized roughened glass surfaces.

I. INTRODUCTION

A cursory examination of a visible laser beam incident on any refracting or reflecting system will show that energy is scattered from the laser beam. This scattering may be due to dust particles, irregularities of the surfaces, or to inhomogeneities in the volume of the material. Depending upon the surface, some energy is scattered at wide angles from the laser beam. A knowledge of the amount of scattered energy is of primary importance in determining the losses and may assist in characterizing the surface.

II. EQUIPMENT

To measure the power lost by scattering and reflection, a probing type detector is desirable. The detecting system must in no way affect the beam propagation and must be able to discriminate and measure the energy flowing across a small but finite area. An ideal probe-detector is visualized here as a single mode optical amplifier and lens system that would respond only to plane waves within a diffraction limited spot in the focal plane of the lens system.

In view of the nonavailability of an ideal probe, an effort has been made to design and fabricate a detecting system which would embody

* Registered trademark of E. I. DuPont de Nemours, Inc.

as many features of the ideal case as possible. For lack of a better name this system will be referred to as a focused optical probe.

The basic elements of the focused probe and its general configuration are shown in Fig. 1(a). By using a lens and mirror system as an adjunct to the detector (an RCA 7102 photomultiplier), well defined measurements can be obtained. As indicated in Fig. 1(a), a mirror has been used to reduce the overall length of the probe and to permit scatter measurements to be made to within a few degrees of an incident beam. An iris centered in the focal plane of the lens nearest the detector acts as a stop which limits the acceptance angle of that lens and provides a small area at the focal point of the second lens for measure-

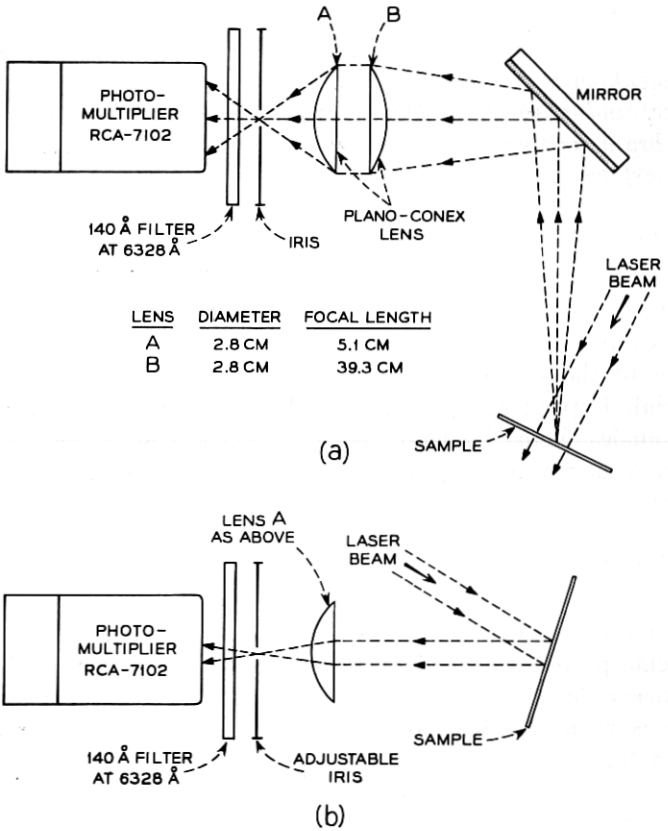

Fig. 1 — Optical probes; (a) focused, for angular scattering measurements, (b) modified for measurement of scattering in the direction of specular reflection.

ment of the power reflected or scattered from a surface placed in that focal plane.

The elements of the probe are assembled in a light-tight housing mounted on a cross-feed indexing table which permits one rotary and two transverse motions for probe positioning. The position of the focal point is indicated by a gauge attached to the mirror housing. Also shown here as Fig. 1(b), is the drawing of the probe modified for measurement of scattering in the specular direction; this modified version is discussed later.

To provide an adequate measuring range in the detection system, a chopper and phase detector are used, as indicated in Fig. 2. With the probe iris set at minimum opening the signal to noise ratio for this equipment is about 75 db using a one-sec. time constant. The dc excited laser (length — 1 meter) is operated at 0.63μ; its cavity mirrors have a radius of curvature of 10 meters and an iris within the cavity is used to suppress higher order modes. Wratten neutral density filters are used at attenuators.

The focused probe response was measured by rotating the focal area of the probe about a fixed point in the laser beam, as indicated in Fig. 3. The measured response is also shown there. The response falls rapidly as θ, the angle between the laser beam and the normal to the focal area of the probe, increases. Also plotted as a dashed curve in

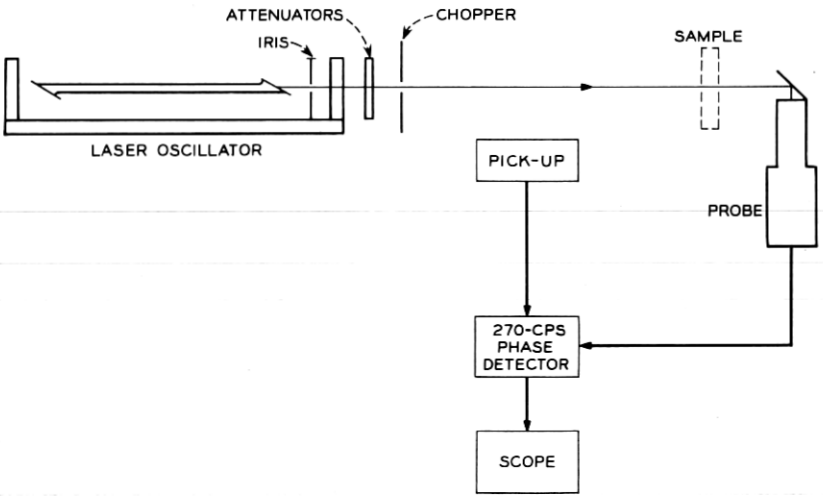

Fig. 2 — Equipment schematic.

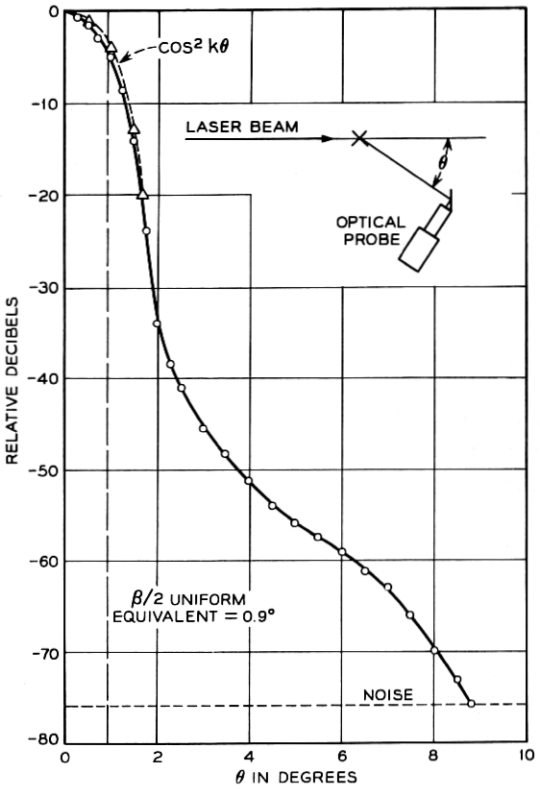

Fig. 3 — Focused probe response curve.

Fig. 3 is the function $\cos^2 k\theta$ which is a reasonable approximation of the measured response (if $k = 50$). Later discussion will be concerned with the idealized case of a uniform distribution over the solid angle of the probe. If the actual response, $\cos^2 k\theta$, is integrated over θ, one can determine the width of the equivalent uniform response; this turns out to be $\beta \cong 2 \times 0.9° = 1.8°$ as indicated in Fig. 3.

III. TEFLON

3.1 *Measurements*

Teflon was one of the first materials to be tested. The measurements indicate that scattering from Teflon is diffuse. They produce a Lambert

type pattern which can be represented reasonably well by a simple mathematical model obeying a cosine law.

The scattering measurements were made as follows: a particular thickness of Teflon was introduced normal to the laser beam (Fig. 2) and probe measurements were made by rotating the axis of the probe about a selected point on the surface of the sample. In the following, a reference to forward scatter means that the measurements were made with the probe situated in the forward hemisphere defined by the direction of propagation of the laser beam whereas back scatter means that these measurements were made with the probe located in the back hemisphere.

Teflon pieces of $\frac{1}{16}$, $\frac{1}{8}$, $\frac{1}{4}$, $\frac{1}{2}$, and of 1-inch thickness were used as samples. As one can see from Fig. 4, where the back-scatter data obtained from several of the samples are plotted (upper curve), any one of the samples can be well represented by the average curve shown there, hence this average curve will be used in what follows. It should be noted that the portion of the curve from $\theta = 175°$ to $\theta = 180°$ was obtained by extrapolation. Also shown in Fig. 4 are the forward scatter data from the one-half inch sample and for comparison, the computed cosine dependence for a Lambert surface (the dashed curve). Since the samples were of finite thicknesses, measurements were not taken out to $\theta = 90°$.

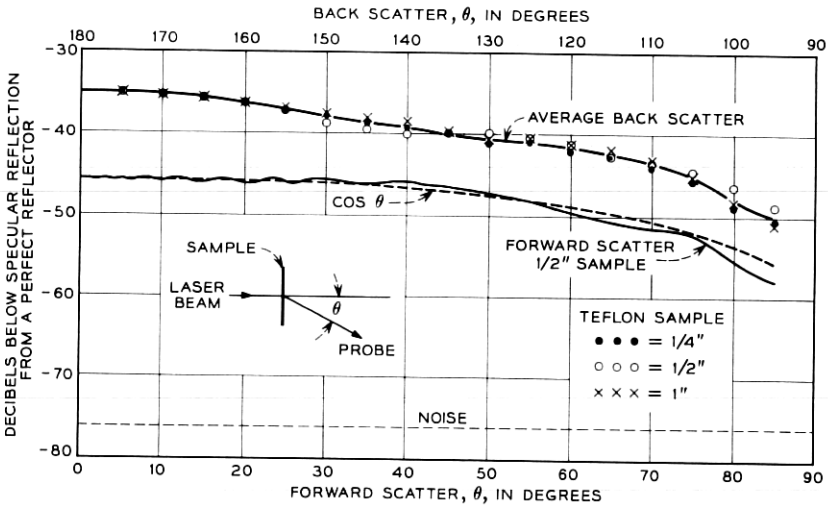

Fig. 4 — Forward and back scatter measurements from Teflon samples.

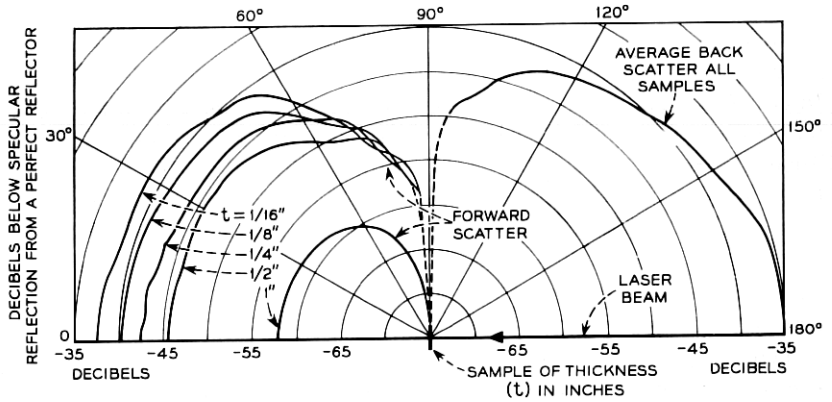

Fig. 5 — Polar plot of scattering from Teflon samples of various thicknesses (t).

Fig. 5 shows both forward and back scatter data for all sample thicknesses as polar plots for ease of comparison.

3.2 *Discussion of the Scatter Model for Teflon*

First, consider unit power incident on the surface of a partially transparent material and assume there is no specularly reflected component[1] from the surface; the energy is either scattered or absorbed. Let $\sigma(\Omega)$ be the scattering coefficient per unit solid angle, then by conservation of energy

$$1 = \frac{1}{4\pi} \int_{4\pi} \sigma(\Omega)\, d\Omega + a \tag{1}$$

where a is the fraction of the incident power that is absorbed in the sample and the integral term represents all of the scattered power, and in this case includes scattering from the volume of the material.

Now, assuming azimuthal symmetry in the scattered power and letting $\sigma(\theta)$ be the scattering coefficient in the direction $\Omega(\theta, \varphi)$, then the power $S_m(\theta)$ accepted by the probe (relative to that which would be received from a suitably oriented perfect reflector) looking to the direction θ^* is

$$S_m(\theta) = \sigma(\theta)\, \frac{\omega_0}{4\pi} \tag{2}$$

where $\omega_0 \cong \beta^2$ is the solid angle of the probe response.

Let $\sigma(\theta) = \sigma_b(\theta) + \sigma_f(\theta)$ where the first and second terms on the

* θ is the angle measured between the laser beam and the normal to the focal area of the probe (Fig. 4).

right represent the back and forward scatter coefficients respectively. Substituting for $\sigma(\theta)$ in (1),

$$1 = \frac{1}{2}\int_{\pi/2}^{\pi} \sigma_b(\theta) \sin\theta \, d\theta + \frac{1}{2}\int_{0}^{\pi/2} \sigma_f(\theta) \sin\theta \, d\theta + a. \qquad (3)$$

From (2), $\sigma(\theta) = 4\pi S_m(\theta)/\omega_0$ and since the measurements are made in both the forward and back scattering directions one writes $S_m(\theta)$ as $S_{mf}(\theta)$ or $S_{mb}(\theta)$. Substituting for σ in (3), one obtains

$$1 = \frac{2\pi}{\omega_0}\int_{\pi/2}^{\pi} S_{mb}(\theta) \sin\theta \, d\theta + a + \frac{2\pi}{\omega_0}\int_{0}^{\pi/2} S_{mf}(\theta) \sin\theta \, d\theta. \qquad (4)$$

From numerical integration of the data, it has become evident that for all Teflon samples, one-half of the incident power is scattered Lambert-wise in the *back hemisphere*, i.e., the first integral of (4) equals one-half. The third term of (4) is evaluated by numerically integrating the data. Subtracting these two terms from unity gives that fraction a of the power absorbed by the sample.

The values for the total power scattered in the forward direction (the third term in (4)) as obtained by numerical integration are tabulated in Table I.

3.3 *Evaluation of Absorption Coefficient*

The power absorbed by the sample is written as

$$a(db) = 10 \log_{10} \exp(-\alpha d) \qquad (5)$$

where α is an absorption coefficient and d the thickness of the sample. Since the total forward scattered power is known from measurements similar to those in Fig. 4, and assuming again that half of the power is available for transmission, the power absorbed by the sample can be determined by solving (5) for α. By using the values given in Table I and averaging the α's obtained from (5), this gives an absorption coefficient for Teflon of $\alpha = 4.7$ inches^{-1} (± 1.1).

TABLE I

Teflon SampleThickness (inches)	Total Forward Scatter
$\frac{1}{16}$	0.38
$\frac{1}{8}$	0.24
$\frac{1}{4}$	0.136
$\frac{1}{2}$	0.085
1	0.005

IV. METALLIC SURFACES

Samples of aluminum, steel, and brass were selected from stock of bulk metals, the only criterion applied in the selection being that the samples be reasonably flat. One side of each sample was cleaned and polished with a liquid metal cleaner. In addition to the bulk metals, a first surface aluminized mirror and three aluminized roughened glass flats were measured. The roughened glass flats were prepared by hand grinding each flat with one of the following grit sizes: 5μ, 12μ, or 25μ. After cleaning, the surfaces were aluminized in vacuo.

Using the focused probe (Fig. 1(a)), angular scattering measurements were made as follows: a particular sample was introduced normal to the laser beam and probe measurements were made by rotating the axis of the probe about a selected point on the surface of the sample, as shown on Fig. 6(a). The minimum angle θ (as measured between the beam and the axis of the probe) at which angular scattering could be measured was about 175°. The measured (angular) scatter data for the aluminum, steel, brass, first surface mirror, and the roughened glass flats are plotted in Figs. 6(a) through 6(d), respectively. The solid curves represent the power measured by the focused probe (normalized to the specularly reflected power the probe would have measured if the sample were replaced by a perfect reflector) for the samples just mentioned as the probe is rotated about the sampling point from $\theta = 175°$ to $\theta = 95°$. The solid dots at $\theta = 180°$ represent the measurements in the specular direction. It should be noted that this value (at $\theta = 180°$) contains both the specularly reflected component as well as the scattered power in the specular direction. The amount of energy scattered in the specular direction is obtained by a modification of the focused probe (Fig. 1(b)), which will be discussed later. With the aid of this second set of data, one can find the specular reflection coefficient for the surface. The data obtained using these two methods permit one to evaluate the total scattered energy.

In Figs. 6(a), 6(b), and 6(c), there are two sets of curves for each side of the metal samples. The curves labelled P and D (without subscripts) represent the polished and dull sides for a given orientation of the sample; the second set (designated by subscript 90) was obtained by rotating the sample 90° about its normal. From these figures, the effects of preferential scattering are readily evident. This type of scattering is due to orientations given to the surface facets as a result of the rolling operations used in processing the bulk metal.[2] As

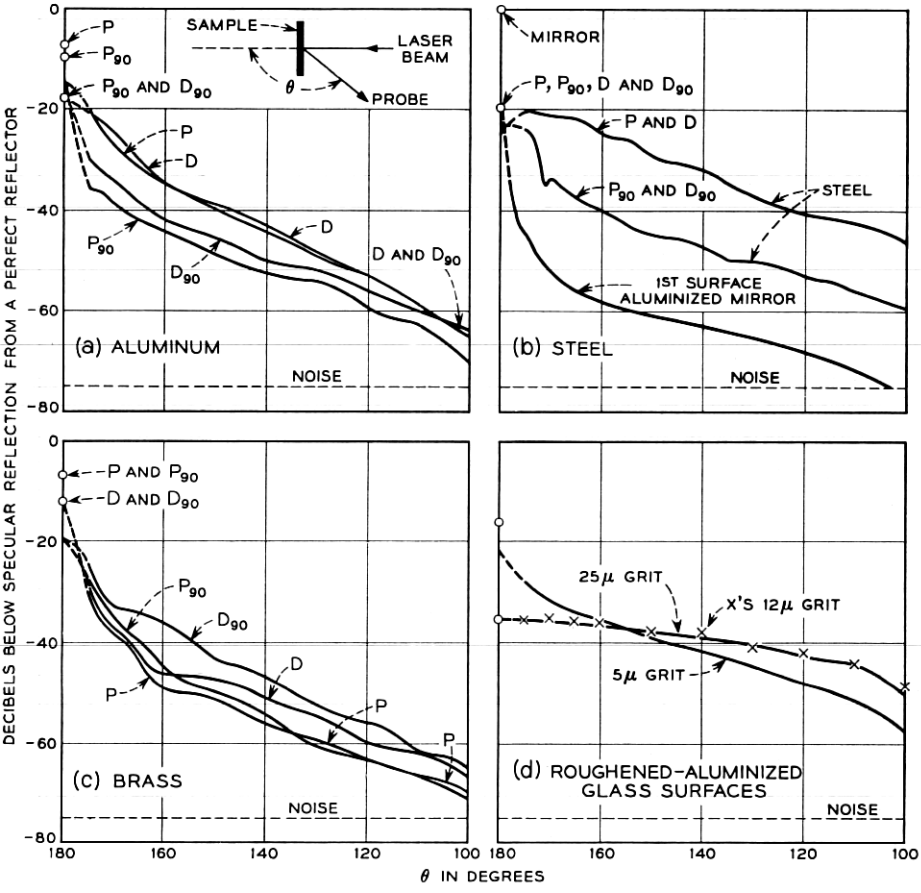

Fig. 6 — Angular scatter measurements for various surfaces. P and D denote the polished and dull side of sample. The subscript 90 denotes a 90° rotation of the sample about its normal. The solid dots at $\theta = 180°$ are total measured values, i.e., they include the specularly reflected component.

the number of rolling operations used to achieve the final metal thickness are increased, the more anisotropic the surface becomes. Also shown in Fig. 6(b), scattering from a first surface mirror is relatively small as expected. From Fig. 6(d), it appears that the 12μ and 25μ grit roughened flats are diffuse scatterers.

It becomes rather apparent after studying these figures that if the scattered energy could be measured in the specular direction, a good approximation of the total scattered energy could be obtained by

smoothly connecting the curve from $\theta = 175°$ to the value obtained at $\theta = 180°$ and then integrating, assuming circular symmetry in the scattered component. A method of measuring scattering in this direction ($\theta = 180°$) will be discussed next.

V. SCATTERING IN THE SPECULAR DIRECTION

If the assumption is made that the energy in the specular direction can be described by a specularly reflected component and an isotropically diffuse component, a method for measuring the scatter in the specular direction presents itself. For this purpose, a single plano-convex lens with a variable iris in its focal plane can be used. Since the specularly reflected component is focused, increase in iris opening* will not change the transmission through the systems and any increase in measured level will be due to the scattering in the specular direction. This increase will be proportional to the iris area provided the scattering in the specular direction is sufficiently diffuse. Operation of such a system can quickly be checked by viewing a plane wave (say the laser beam) directly in which case the energy measured will be constant, i.e., independent of iris openings, whereas for a perfectly diffuse surface, the energy measured would obey a square law in the diameter d of the iris.

The focused optical probe (Fig. 1(a)) discussed above has been modified to permit its use in measuring this scattering in the specular direction. As shown in Fig. 1(b), this modification is accomplished by merely removing the mirror and lens B. Measurements looking directly at the laser beam using the modified probe (Fig. 1(b)) show no appreciable change in level as the iris opening is varied from minimum to maximum. To check the square law performance of the system, scattering from a teflon surface was measured — since previous measurements (Section III) had shown it to be a very diffuse scatterer. The data obtained from the Teflon sample are shown as a solid curve in Fig. 7; these, when compared with the calculated (dashed) square-law curve, indicate that the system responds properly to a completely diffuse field.†

* Iris openings much larger than the diffraction limit of the lens are considered here.

† In some cases, it was necessary to use an incident beam larger in diameter than the normal laser beam. A lens combination was used to obtain the desired beam magnification. Measurements of the response of the modified probe to this enlarged beam show a slight increase of 0.3 db in measured power as the iris opening is increased from 0.02-inches diameter (minimum) to 0.14-inches diameter (maximum). This increase is attributed to scattering in the lenses used to enlarge the beam and has negligible effects on the measurements.

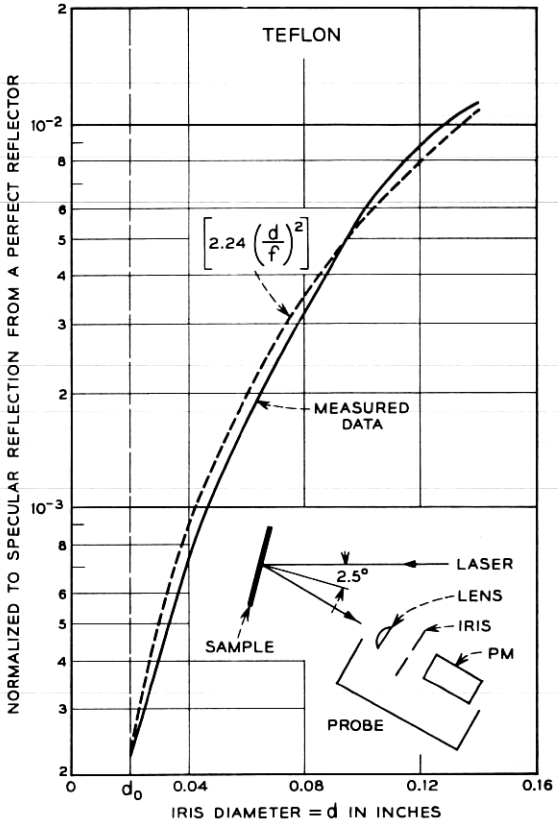

Fig. 7 — Scattering from Teflon in the direction of specular reflection.

With the above tests providing a degree of assurance in the probe's performance, scattering measurements in the specular direction as shown in Fig. 7, were made on the samples discussed in Figs. 6(a)–6(d). These data are shown as Figs. 8(a)–8(f). Here the solid curves represent the measured data and the dashed curves are calculations based upon the model that the measured power S_m* contains both a specularly reflected component R_{0m} and a scattered component $c(d/f)$,^{2} where d is the diameter of the iris opening and f is the focal length of the lens. The constants of the equation $S_m = R_{0m} + c(d/f)^2$ are determined by fitting to the measured data. In reality, R_{0m} is the specular reflection coefficient for the surface. The parame-

* Normalized to the power specularly reflected from a perfect reflector.

ter, c, for the samples in Figs. 8(a)–8(f) is the relative scattered power per unit solid angle in the specular direction.

An examination of Figs. 8(a)–8(f) shows reasonable agreement between measured data and calculated values (always so for small values of d, where the curves were fitted); however, for those surfaces with a significant reflection coefficient (for example Fig. 8(a) for polished aluminum) the model predicts a larger value* than that measured for larger values of d. This effect is attributed to a preferred scattering in the specular direction by the individual surface facets. In Fig. 8(a), the point of divergence of the measured and fitted curves for polished aluminum occurs at $d = 0.08$ inches; the corresponding planar acceptance angle of the probe at this iris opening is $\beta = d/f = 0.04$ since f is two inches. Now it follows from elementary diffraction theory that if D is the dimension of an aperture (in this case a "reflecting" surface facet) and λ the wavelength of radiation, then the angle within which the radiation from this facet is concentrated is $\alpha = \lambda/D$. From the data in Fig. 8(a), one is therefore led to the conclusion (letting $\alpha = \beta$) that the facet dimension is $0.63\mu/0.04 = 16\mu$. Microscopic examination of the surface indicated an average facet size of about 40μ for the aluminum sample.

The specular reflection coefficients, R_{0m}, for all surfaces on which specular scattering measurements were made are tabulated in Table II.

The value given here for the specular reflection coefficient of a first surface aluminized mirror is about 10 per cent larger than the value usually quoted for aluminum film. Similarly there are differences in reflection coefficient for those samples listed with the (1.) and (2.) notation in Table II. Provided there are no polarization effects occurring at the surface facets, these specular reflection coefficients should be the same because the sample is merely rotated 90° about its axis in these two conditions.

Scattering in the specular direction having been determined, the scattering in the direction $\theta = 180°$ can now be plotted on the angular scattering curves, Figs. 6(a)–6(d); in those figures, the value at $\theta = 180°$ is joined to the angular scatter curve at $\theta = 175°$ by the dashes. This complete curve then represents the scattered energy as a function of θ. If circular symmetry obtains, a numerical integration yields the total scattered power.

* It should be noted that the calculated curves in some cases (e.g., Figs. 8(a), 8(d), and 8(e) exceed unity; this is because the square law dependence on iris opening assumes isotropically diffuse scattering from the facets which, of course, is not true if the facets have directivity.

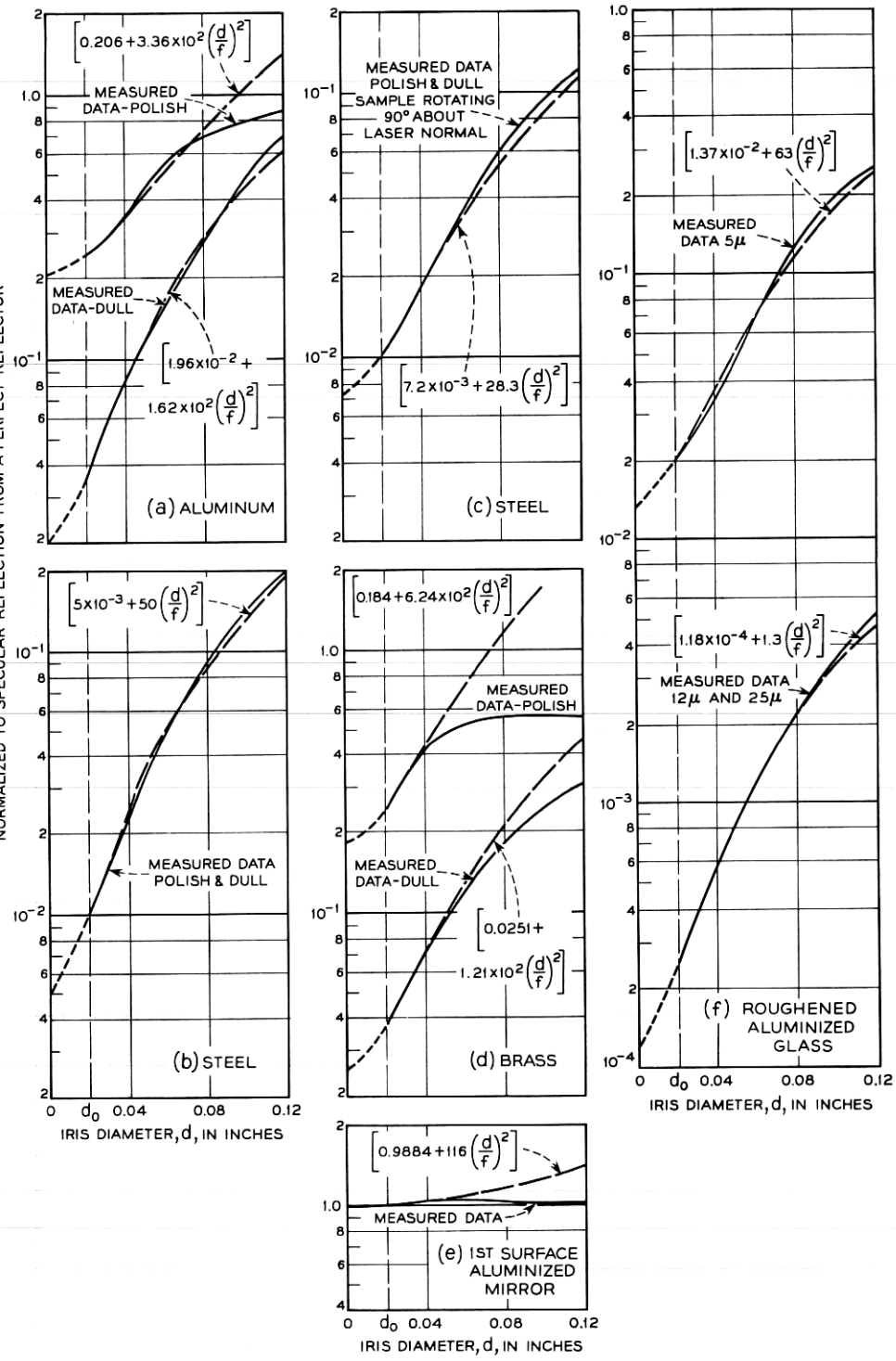

Fig. 8 — Scattering from various metallic surfaces in the direction of specular reflection.

TABLE II

Material	Specular Reflection Coefficient R_{0m}	Scattering in Specular Direction for an Iris Opening of d_0
Alum. Polish	0.21	0.034
Alum. Dull	0.02	0.016
Steel (polished & dull) (1)	5×10^{-3}	5×10^{-3}
Steel (polished & dull) (2)	7.2×10^{-3}	2.83×10^{-3}
Brass Polish	0.18	0.062
Brass Dull	0.025	0.012
1st Surface Mirror	0.988	0.012
5μ Roughened Glass Aluminized	0.014	6.3×10^{-3}
12μ & 25μ Roughened Glass Aluminized	1.2×10^{-4}	1.3×10^{-4}
Nickel Foil	0.97	0.032
Beryllium Copper-Polish (1)	0.013	0.031
Beryllium Copper-Dull (1)	5.5×10^{-3}	5.5×10^{-2}
Beryllium Copper-Polish (2)	0.016	0.014
Berylllium Copper-Dull (2)	6.5×10^{-3}	2.7×10^{-3}

Note: (1.) preferential scatter in plane of probe.
(2.) preferential scatter 90° to plane of probe.

VI. DISCUSSION OF THE SCATTERING MODEL FOR METALLIC SURFACES

First, consider unity power incident on an opaque (but otherwise arbitrary) surface. This power, reflected in the specular direction in proportion to the specular reflection coefficient, R_0, of the surface, is scattered over the hemisphere, or absorbed. Let $\sigma(\Omega)$ be the scattering coefficient of the surface in the direction Ω, then by conservation of energy,

$$1 = R_0 + \frac{1}{2\pi} \int_{2\pi} \sigma(\Omega)\, d\Omega + a \tag{7}$$

where a is the fraction of incident power absorbed by the surface and the integral term represents all the scattered power in the hemisphere.

Assuming azimuthal symmetry in the scattered power and letting $\sigma(\theta)$ be the scattering coefficient in the direction $\Omega(\theta, \sigma)$ then the power accepted by the probe looking toward the direction θ is (as in Section III) $S_m(\theta) = \sigma(\theta)\omega_0/4\pi$, the relative power measured by the probe looking toward the direction θ being designated by $S_m(\theta)$. Substituting for σ and $d\Omega$ in (7), one obtains

$$1 = R_0 + a + \frac{4\pi}{\omega_0} \int_{\pi}^{\pi/2} S_m(\theta) \sin\theta\, d\theta = R_0 + a + S_{TM} \tag{8}$$

where S_{TM} is the *total* scattered power. As previously stated, the acceptance angle of the focused probe is $\omega_0 = 10^{-3}$ steradians, thus when the

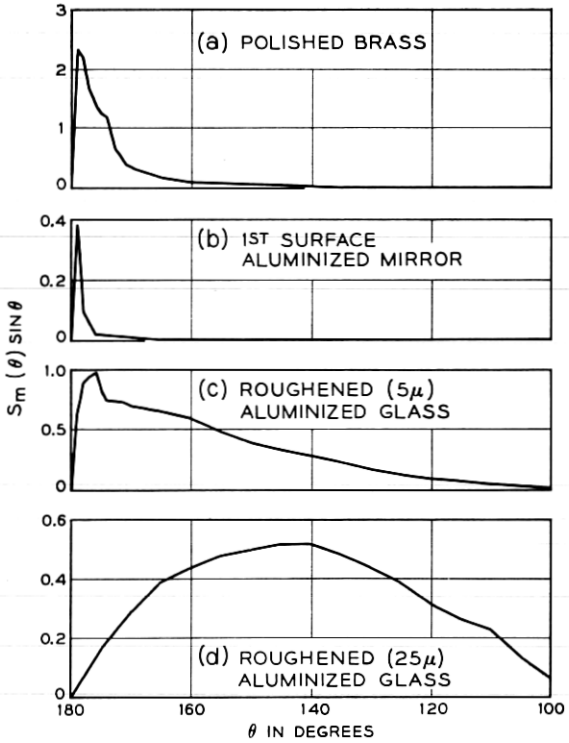

Fig. 9 — Integration curves for evaluation of total scattered power.

integral has been numerically evaluated, the fraction of power a absorbed by the surface can be determined.

The development of (8) assumed azimuthal symmetry whereas an examination of the scatter curves of Figs. 6(a)–6(c) shows these surfaces to be (in varying degrees) anisotropic; however, it is instructive to consider the curves representing the polished brass surface (Fig. 6(c))

TABLE III

Material	Measured Specular Reflection Coefficient R_{0m}	Measured Total Scattering Coeff. S_{TM}	Derived Absorption Coeff. (a)
Brass	0.18	0.44	0.38
1st Surface Mirror	0.988	0.01	0.0016
5μ Glass	1.4×10^{-2}	0.91	0.076
25μ Glass	1.2×10^{-4}	0.97	0.03

since the two curves* taken in the two azimuth planes are reasonably similar so that the symmetry is fairly good. A numerical integration of this curve yields a total scattered power of 0.44. The curve used for the numerical integration (the integrand of (8)) in this case is shown in Fig. 9(a).

In addition to the brass sample, numerical integrations of scattering have been made for the 1st surface mirror (Fig. 6(b)) and the roughened glass flats (Fig. 6(d)). Since the 12μ and 25μ roughened glass flats have similar scatter curves only the data for the 25μ glass sample was integrated. These data are given in Table III, along with the absorption coefficient a, as derived from (8).

The curves used for the numerical integration of the power scattered from these surfaces are shown in Fig. 9. Here one notices that the largest contribution from the mirror peaks around 179° and that the major contribution occurs in the first few degrees, whereas the curve for the 5μ glass has a decided peak occurring around 176° and has significant values out to fairly wide angles. The curve for 25μ glass peaks at about 140° since it is a very diffuse scatterer.

VII. CONCLUSIONS

Based upon the measurements, it would appear that an optical probe, with modifications to permit measuring scatter in the specular direction, is a useful tool for obtaining information on scattering from an arbitrary surface. The combination of angular scatter and specular scatter measurements have been successfully used in determining the total scattered power from an arbitrary surface. The method of measuring scatter in the specular direction has also produced values for the specular reflection coefficient and the absorption coefficient. Certain conclusions about facet size and the nature of the scattering process have been obtained from these data.

VIII. ACKNOWLEDGMENT

The interest and helpful suggestions of D. C. Hogg are greatly appreciated.

REFERENCES

1. Beckman, P., and Spizzichino, A., *The Scattering of Electromagnetic Waves from Rough Surfaces*, The Macmillan Co., 1963, p. 89.
2. Barrett, C. S., *Structure of Metals*, McGraw-Hill Book Co., 2nd Edition, Chap. 18, 1952.

* Curves such as these are examples of the $S_m(\theta)$ in (8).